Ocean Engineering 260 (2022) 111936

Contents lists available at ScienceDirect

Ocean Engineering

journal homepage: www.elsevier.com/locate/oceaneng

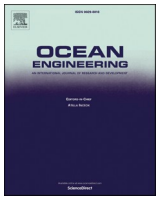

Simulation of the impact of parameter manipulations due to cyber-attacks and severe electrical faults on Offshore Wind Farms

Nikolai Kulev *, Frank Sill Torres

German Aerospace Center (DLR), Institute for the Protection of Maritime Infrastructures, Department for Resilience of Maritime Systems, Fischkai 1, 27572, Bremerhaven, Germany

ARTICLE INFO

Keywords:
Offshore wind farm
Power system dynamics
Disturbance impact
Cyber-attacks
Power system security
Safety

ABSTRACT

Motivated by the transition to renewable energies in the context of ongoing climate change, offshore wind energy is of rising importance for the energy provision on national and international level. This trend, though, puts pressure on the safety and security community to provide appropriate analyses and solutions in regard to safety and security threats. Based on this motivation, this work investigates the internal disturbances in Offshore Wind Farms (OWF) provoked by cyber-attacks and severe electrical faults that might lead to high impact events. Therefore, the influences of these disturbances are quantified using a simulation model that represents electrical and mechanical aspects as well as the protection and control system. Furthermore, the dependence of the system response on to the disturbance characteristics is determined and the critical values of the disturbance characteristics leading to the OWF service interruption or even physical damage are identified. The results indicate in quantitative manner processes in the electrical and mechanical systems during parameter manipulations due to cyber-attacks and severe electrical faults. This, together with the quantitative signatures of the disturbances, enable future improvements of the security and stability of OWF systems.

1. Introduction (Background and motivation)

Offshore Wind Energy (OWE) exhibits a continuous increase of its share within overall power supply. For example, in 2020 OWE contributed with 4.9% to the overall energy production in Germany.[1] Worldwide initiatives, e.g. the planned enormous 25-fold expansion of Europe's offshore wind capacity to 300 GW in2050,[2] indicate the continuous increase of the importance of OWE. This trend turns OWE systems into critical infrastructures with its impact on the power grid dynamics and reliability (Wu et al., 2019), accompanied by rising complexity and sophistication.

Recent high-impact low-probability (HILP) disturbance events in Offshore Wind Farms (OWFs) underline this assumption, both through the direct impact of disturbances and through the decision-making process on management or regulatory level. A lightning strike on August 9, 2019 on the transmission network and the following simultaneous shutdown of a gas-fired power plant and the Hornsea OWF led to a nearly 1-h power-down affecting more than 1 Million consumers in Great Britain after the activation of the automatic protections.[3] The energy production of the Alpha Ventus OWF near the German North Sea, providing power for about 68,000 households, was reduced to half after a substantial part of the nacelle housing of a wind turbine fell into the sea on April 6, 2018. As a precaution, the remaining wind turbines (WTs) of the same type were put into idling mode (no power generation) for inspection even for weeks after the accident.[4]

Due to the coupling between physical systems, i.e. power generation, and cyber systems, i.e. information and communication, wind farms are considered to be cyber-physical systems (Kröger and Zio, 2011), (Wu et al., 2019), (Yan et al., 2011), (Ahmed and Kim, 2017). Accordingly, the power system dynamics and the required performance of wind farms arise from intricate, often nonlinear interactions among a large number of interconnected and spatially/geographically distributed components of different types and from different domains, i.e. physical and cyber, with different time scales, non-linear behavior and feedback loops

* Corresponding author.
E-mail addresses: Nikolai.Kulev@dlr.de (N. Kulev), Frank.SillTorres@dlr.de (F.S. Torres).

[1] https://www.bdew.de/media/documents/20210322_D_Stromerzeugung1991-2020.pdf.
[2] https://ec.europa.eu/commission/presscorner/detail/en/ip_20_2096.
[3] https://www.theguardian.com/business/2019/aug/16/national-grid-blackout-report-avoidable-faults-blamed.
[4] https://w3.windfair.net/wind-energy/news/28299-alpha-ventus-nacelle-nacelle-housing-damage-repair-offshore-wind-farm.

https://doi.org/10.1016/j.oceaneng.2022.111936
Received 14 January 2022; Received in revised form 23 May 2022; Accepted 4 July 2022
Available online 5 August 2022

(Kröger and Zio, 2011). Therefore, wind farms become exposed and vulnerable to many failures/faults and attacks occurring with certain probability, as typical for critical infrastructures, engineering and cyber-physical systems (Kröger and Zio, 2011), (Khaitan and McCalley, 2015). Furthermore, the normal operation of such systems does not allow to detect 'hidden' interactions between the system elements which might become crucial for the evolution of failure events - the dynamic degradation is sensitive to parameter variations (Kröger and Zio, 2011).

A failure/fault or an attack within a windfarm would cause transients within its power system dynamics, i.e. the power flow of the affected component would be redistributed to other components according to circuit laws, and subsequently redistributed again according to automatic, manual control and protection actions (Kröger and Zio, 2011). These transients include deviations of power flows, frequency, currents and voltages accompanied by the corresponding operation or maloperation of protection devices, controls, operator procedures and monitoring and alarm systems, resulting eventually in component disconnection or network topology change (Kröger and Zio, 2011). Therefore, the influence of the cyber systems on the power system dynamics of wind farms (Yan et al., 2011) would result in cyber threats potentially leading to abnormal operation and undesired tripping of WTs (Wu et al., 2019).

The above-mentioned deviations are related to the fundamental definition of power system security, according to which a power system is considered to be secure if it remains stable after the occurrence of a disturbance due to a contingency (Kundur et al., 2004), (Machowski et al., 2011). Furthermore, the deviations due to the disturbance shall not result in equipment overloads or violations of physical/operational constraints, e.g. voltage or current (Kundur et al., 2004), (Machowski et al., 2011). In specific terms, the security of a power system is defined in (Kundur et al., 2004) as the degree of risk in its ability to survive imminent disturbances (contingencies) without interruption of customer service (Machowski et al., 2011). In this way, the power system security is related to the robustness of the system to imminent disturbances considering physical constraints or requirements as well.

The contingencies under consideration include damages to equipment, such as an explosive failure of a cable or the fall of transmission towers due to ice loading or sabotage, i.e. both unintentional or random events, failures and events of intentional origin are considered (Kundur et al., 2004). Accordingly, power system security combines the aspects of safety and security usually used in the literature. Safety relates to the absence of harm to users, the public and the environment due to unintentional or random events, failures or faults. In contrast, security means the absence of harm due to events of intentional origin such as sabotage, cyber-attacks and terrorism (Kröger and Zio, 2011), (Aven, 2018).

Ackermann et al. (Ackermann, 2012) pointed out two basic abilities related to the power system security of OWFs: (1) the ability to supply the electrical demand of the customers at all times, and (2) the ability of the power system to withstand sudden electrical disturbances, e.g. due to short circuits or unanticipated loss of system elements. However, the above-mentioned definition of power security goes beyond the electrical disturbances. Therefore, detailed knowledge and understanding of the behavior under disturbed operating conditions is needed regarding the OWF power system security. This also requires the investigation of OWF as a whole and the assessment of the vulnerability of OWF to HILP events, both from safety and security perspective (Kröger and Zio, 2011), (Panteli and Mancarella, 2017). Additionally, the Fault Ride-Through (FRT) capability, which enables WTs to remain connected to the transmission networks in the presence of electrical faults in the power system, must be considered (Ackermann, 2012), (Schaffarczyk, 2014), (Anaya-Lara et al., 2014).

The dependence of deviations, measured as performance degradation, under disturbed conditions on the disturbance severity or characteristics is investigated in (Panteli and Mancarella, 2017). The authors conclude that the higher the disturbance severity, the bigger degradation, i.e. highly severe disturbance lead to the system state of biggest degradation, regarding electrical disturbances in power systems in terms of short-term resilience of power systems. The authors discuss five possible system states of power systems that are based on the degree of the violation of operational and physical constraints, corresponding to different degradation and the short-term resilience, respectively. It is noted that the transition between these states depends on the severity of the electrical disturbance, i.e. its characteristics, and the effectiveness of the control actions, emphasized also by (Sansavini, 2017) in this cotext. These conclusions illustrate the dependence of the power system dynamics caused by the disturbance on the disturbance characteristics (disturbance sensitivity).

In this work, we investigate in the context of OWF the impact of disturbances due to manipulations of the automated control and protection actions, caused by cyber-attacks, and due to severe electrical faults. The main goal is the quantification of the impact of these disturbances with a dynamic simulation model of the OWF power system – at one hand from a safety and security perspective, and on the other hand regarding both non-electrical and electrical disturbances, i.e. in terms of power system security (Kundur et al., 2004). Therefore, the dependence of the system response to the disturbance characteristics is analyzed and the critical values of the disturbance characteristics leading to a service interruption, e.g. undesired tripping of WTs, or even physical damage of the elements of the OWF are identified. The obtained results provide quantitative signatures of the disturbances, which enable future improvement of the security and stability of OWF systems.

A further aspect is the application of the Disturbance Impact Index (DII), which relates the deviations (due to the disturbances) to the disturbance characteristics, i.e. location and duration, and system properties, i.e. generator inertia constant. Consequently, this indicator enables measuring the OWF sensitivity to disturbances as a relation between system response in terms of deviations, i.e. disturbance impact, and disturbance characteristics, such as duration or location. In this way, the aspect of fault propagation within the OWF system is included as well. Because the DII considers both fault sensitivity and propagation it can also be regarded as a vulnerability/safety-level indicator for a quantitative assessment of the OWF vulnerability to the safety-related disturbances, beyond a typical electrical fault analysis.

The rest of this paper is structured as follows. Section 2 relates to the state of art, while Section 3 proposes methodology for disturbance analysis of the OWF power system. Section 4 presents the obtained simulation results and discuss the application of the disturbance impact index. Finally, Section 5 concludes this work.

2. Preliminaries

This section presents preliminary information that support the understanding of the rest of this contribution.

2.1. OWF power system

Fig. 1 depicts the top-level scheme of the power system of a generic OWF (Ackermann, 2012), (Anaya-Lara et al., 2014), (Ng and Ran, 2016), (Fernández-Guillamón et al., 2019), (Perveen et al., 2014). At the left-hand side is an array of Wind Turbines (WTs) interconnected through internal AC subsea cables. The active power P generated by the WTs through the conversion of mechanical energy from the wind into electrical energy is transmitted via these cables to the offshore substations, while the reactive power Q flows in the opposite direction. The substations operate as step-up transformer/converter combination if a DC export cable is used (dashed box), or as a step-up transformer if an AC export cable is used (solid box). In this way, the voltage level of the WT array is increased to the voltage level of the export cable in order to transmit the energy to the shore, with inversion to DC if a DC export cable is used. The undersea export cable system is also connected to the onshore substation, which operates as a converter/step-up transformer combination or a step-up transformer, respectively. The inversion to AC

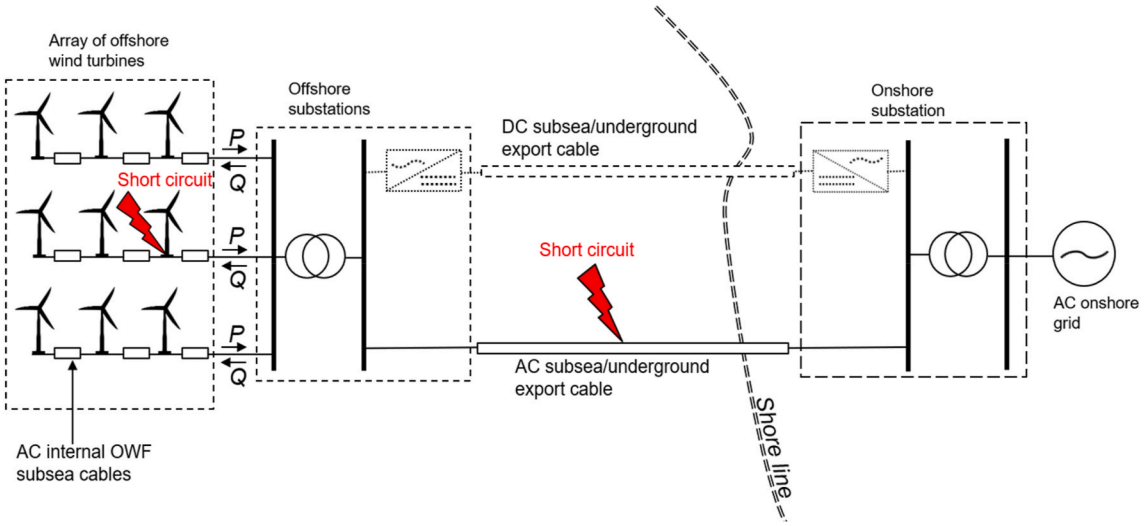

Fig. 1. Power system model of a generic OWF with the relevant electrical disturbances for this work.

is performed if a DC export cable is used and the voltage level is increased to the level of the AC onshore grid. The generated power by the WTs is fed into the grid at the grid connection point. In the case of AC connection both the OWF and onshore grid must be synchronized (must have the same frequency) whereas in the case of DC export cable the onshore AC grid and OWF, i.e. the array of offshore WTs connected with AC internal cables, can have different frequencies.

The main aspects directly related to the OWF power system depicted above have been extensively investigated, with the current status and future trends summarized in (Fernández-Guillamón et al., 2019), (Perveen et al., 2014). The *energy conversion and transmission* systems on both wind turbine and wind farm level are the backbone of the OWF power system. The arising issues (e.g. efficiency, functionality) are addressed in (Ackermann, 2012), (Anaya-Lara et al., 2014), (Ng and Ran, 2016), (Fernández-Guillamón et al., 2019), (Perveen et al., 2014), (Liserre et al., 2011), (Njiri and Soeffker, 2016), (Kumar and Chatterjee, 2016), (Negra et al., 2006), (De Alegría et al., 2009), (Chou et al., 2012), (Erlich et al., 2013). *Stability* (in terms of rotor angle, voltage and frequency) is defined as "the ability of an electric power system, for a given initial operating condition, to regain a state of operating equilibrium after being subjected to a physical disturbance, with most system variables bounded so that practically the entire system remains intact "(Kundur et al., 2004). It is therefore fundamental for the efficient and secure operation of the OWF power system. Accordingly, it is investigated at wind turbine and OWF level in (Ackermann, 2012), (Anaya--Lara et al., 2014), (Ng and Ran, 2016), (Holdsworth et al., 2001), (Erlich et al., 2009). The operation of the *energy conversion and transmission system* demands corresponding *control and protection* systems WT/WF level (Ackermann, 2012), (Anaya-Lara et al., 2014), (Ng and Ran, 2016), (Liserre et al., 2011), (Njiri and Soeffker, 2016), (Kumar and Chatterjee, 2016). The OWF power system is connected to and interacts with the onshore grid. Accordingly, it must comply with the grid requirements. The corresponding issues of *grid impact, interaction and compliance* are investigated, predominantly in terms of power quality and stability, in (Ackermann, 2012), (Anaya-Lara et al., 2014), (Ng and Ran, 2016), (Erlich et al., 2009), (Bolik, 2008), (De Decker et al., 2012). However, the power system must also survive disturbances not classified as stability problems, such as damage to equipment or sabotage as mentioned above, i.e. power system *security* goes beyond mere system stability. This means that the power system may be stable following a contingency, yet insecure due to the fault and post-fault system conditions resulting in violation of operational constraints or equipment overloads, leading eventually to service interruption or damage (Kundur et al., 2004), (Machowski et al., 2011). The current work presents a power system security analysis of the OWF regarding internal HILP disturbances from natural events and malicious acts. So, this work distinguishes itself from the investigations of the impact of grid disturbances on the power system security of the OWF (Arthur et al., 2008) and of the OWF impact on the power system security of the grid (Wu et al., 2010).

Various electrical disturbances can occur within the OWF system: short circuits in the AC or DC grid, load loss, disconnection of transmission cables, loss of other system elements such as a substation, transformer failure and commutation failure at the converter when line-commutated converters (LCC) are used (Ackermann, 2012), (Fernández-Guillamón et al., 2019), (Perveen et al., 2014). These electrical disturbances cause step changes of system parameters, e.g. voltage, topology or load, which result to the transient behavior under disturbed conditions. Accordingly, these disturbances can affect the power system security of the OWF according to the aforementioned definition by (Kundur et al., 2004). The two electrical disturbances investigated in this work are short circuits at the WT terminal and at the AC export cable, both highlighted in Fig. 1.

The time scales of the duration of electrical disturbances regarding control and protection system action range from ms to s (Anaya-Lara et al., 2014). Accordingly, the typical settings of the electrical protection systems as tolerable fault durations and the FRT requirements are in this range, too (Ackermann, 2012), (Schaffarczyk, 2014), (Anaya-Lara et al., 2014).

2.2. Related works

Only a few articles address the cyber-physical effects related to the cyber-attacks of WF regarding infrastructure/equipment safety. The authors in (Staggs et al., 2017) present cyber-physical attack scenarios that have the potential of service interruption on wind farm and substation level. Yan et al. (2011) estimate the impact of cyber-attacks through parameter manipulations through dynamic simulations with the tool DIgSILENT of a single doubly fed induction generator (DFIG) WT connected to the grid. The authors discuss that this could lead to a WT interruption of service, WT overspeed and even equipment damage. However, an investigation of the impact of the manipulation within large-scale wind farm systems, such as the ones discussed in this work, is still missing, not to mention the investigation of impact of the manipulation of a single WT on the remaining WTs in the wind farm. No related investigation has been done using squirrel-cage induction generators (SCIGs) either, despite their share of 48.11% offshore in 2012 (Zhang et al., 2013).

The indicator driven investigation of the impact of the disturbance

characteristics on the power system caused by the disturbance is done in (Eremia and Shahidehpou, 2013), (Preda, 2016). This impact is quantified by the disturbance impact index (DII) by relating the impact of the disturbance on the distributed generators in the system and the disturbance characteristics, i.e. duration, location and type. Dynamic simulations were employed for the impact assessment in (Preda, 2016) using DIgSILENT. No simulation analysis of internal OWF faults based on the DII has been done yet.

2.3. Previous works of the authors

We presented and discussed in Kulev et al. (2019) a functional model of a generic OWF as a cyber-physical system as a network of interacting components, which process and exchange physical quantities, data and signals. The components are grouped into several interacting sub-systems: energy conversion, data acquisition for control and monitoring, data acquisition for protection and maintenance, control and monitoring, protection and maintenance. In this way, the model represents the operation and functionality of an OWF.

Through the functional model, a qualitative investigation of the impact of disturbances due to manipulations by two main scenarios of cyber-physical attacks was performed. The first scenario, which is investigated quantitatively in the present work through simulations, considers the manipulation of the WT mechanical control system by imposing a minimal value of the pitch angle. Alongside with this, the threshold of the rotor speed limit in the protection system is either removed or excessively increased. The consequence would be an abnormal rotor overspeed under normal wind conditions causing extreme mechanical overloads propagating first to the drive-train and the nacelle and then to the WT tower and the transition piece, respectively. Excessive damage and even destruction of the main components would be imminent and the destruction of the structures, e.g. nacelle, tower or transition piece, is possible, accompanied by loss of generated power of the WT.

2.4. Main contributions of the current work

The key problem by the assessment of the impact of the disturbance within the OWF is the determination of the failure system dynamics due to the disturbance of a network of interacting cyber-physical components with feedback loops and non-linearities (Kröger and Zio, 2011), (Khaitan and McCalley, 2015). One qualitative methodology for the purpose is the Failure Mode and Effect Analysis (FMEA), through which an assessment of the propagation of the effect of single sub-system or component fault/failure behavior on the system behavior is performed (Häring et al., 2017). Our previous work (Kulev et al., 2019) was a FMEA study of OWF manipulations, bearing so all the limitations of the qualitative nature of FMEA, e.g. impossibility for the determination of the transients of voltages, currents and power (with their redistribution) by the disturbance simultaneously with the consideration of feedback loops and non-linearities (Kröger and Zio, 2011).

Accordingly, dynamical numerical models and simulations are needed for the determination of the violations of these and other relevant physical quantities for the investigation of the OWF manipulations in terms of a power system security analysis. Such kind of simulations were performed in (Yan et al., 2011) for the assessment of the impact of manipulations. However, there are several limitations regarding this study. The numerical model does not represent a large-scale wind farm system, as the authors themselves state, since only a one WT (DFIG) is used and no modelling of the corresponding cables (export and internal) is implemented for the connection to the grid. The study is also restricted only to manipulations with a duration of several seconds without investigation if the effect is only with transient or also steady state character.

One main contribution of our study is that it overcomes the above-mentioned limitations of (Kulev et al., 2019) and (Yan et al., 2011). For determination of the failure system dynamics due to manipulations, and disturbances in general, we employ dynamical simulation models with the characteristics of large-scale OWF systems such as explicit modelling of the cables (25–30 km export and 1 km internal ones) and including more than one WT (SCIG). Accordingly, we investigate the impact of the manipulation of an individual WT on its service and on the service of the remaining WTs. Additionally, we investigate long-term manipulations durations of 1.67 min (100 s), i.e. about 20 times longer than in (Yan et al., 2011).

The novelty regarding the models and the methodology is transferred to the results and the insights of the current work. Several main contributions in this respect are given by the current work. The fundamental novelty compared to both (Kulev et al., 2019) and (Yan et al., 2011) is that we investigate the manipulation of an individual WT and the interaction between manipulated WT and remaining WTs within the OWF. The manipulation exploits a weakness due the unique design feature of the SCIG that the same mechanism, i.e. pitch angle regulation, is used for both the control of the extraction of mechanical power from wind and the control of electrical power generation. This strong and direct coupling of the electrical system to the mechanical system enables the occurrence of abnormal values of the generated power and of the electrical quantities by the abnormal operation of the mechanical power extraction, e.g. the pitch angle manipulations of a single WT considered here. The manipulation turns the manipulated WT generator practically into a motor consuming power, i.e. generating negative power, and the corresponding abnormal values of the electrical quantities propagate within the OWF so that the remaining WTs get tripped due to limits violation of electrical quantities. This interaction, which does not manifest itself under normal operating conditions, between the WTs under the disturbed conditions of the manipulation alongside with the resulting interruption of service of the whole OWF (Hornsea1[5]) is truly non-trivial and a novelty. This is also an example how the current work extends the results from (Kulev et al., 2019) and (Yan et al., 2011), where the assessment of the manipulation impact suggests that only the mechanical quantities are affected. We observe that the manipulations have an impact on electrical quantities as well, leading to the aforementioned OWF service interruption with SCIG WTs and DC-link overvoltage in DFIG case associated with new threats, such as overheating and fire. Besides we observe a sustained (steady-state) overspeed as a long-term event, suggested but not observed in (Yan et al., 2011).

Our application of the disturbance impact index (DII) differs significantly from its application in (Eremia and Shahidehpou, 2013) and (Preda, 2016) as a means for the identification of coherent generators. Instead we use the DII as means for quantitative specification of the level of the operational (un-)safety of the power system in dependence on the disturbance characteristics and the corresponding power deviation of the WT generator. In this way the highest DII values determined through the simulation results correspond to the lowest level of safety where any additional disturbance would lead to WT service interruption due to violation of operational limits.

3. Materials and methods

In this work, we employ a quantitative methodology for the investigation of disturbances within OWFs. This includes both the implementation of a numerical simulation model of the OWF that is capable of capturing the transient behavior caused by the disturbances (Section 3.1) and an appropriate indicator for the analysis of this behavior (Section 3.2).

[5] https://www.theguardian.com/business/2019/aug/16/national-grid-blackout-report-avoidable-faults-blamed.

3.1. Modelling and simulation of the OWF and disturbances

Modern power generation systems are combinations of electrical circuits and electrical components, electromechanical components (e.g. motors and generators), power electronics components, control systems alongside with corresponding protection systems. Consequently, the resulting system behavior is so non-linear that the only way to understand it is through simulation. Therefore, the results of this work have been obtained by using Simscape™ Electrical™ Specialized Power Systems within the MATLAB/Simulink environment (Perelmuter, 2017), (MathWorksa), (MathWorksb).

The employed models correspond to the OWF functional model presented in Kulev et al. (2019). Thus, the OWF is modelled as a dynamical multi-domain system, described by differential-algebraic equations, consisting of interacting sub-systems of components for energy conversion and transmission, measurement, control and protection. This enables the simulation of the transient system response of the whole OWF to disturbances in the different sub-systems, considering the coupled dynamics of all sub-systems. The models are dynamical cyber-physical representations of the OWF through the interaction of physical quantities, i.e. electrical and mechanical, and information, i.e. data and signals. In our models the spatial dependence of the system

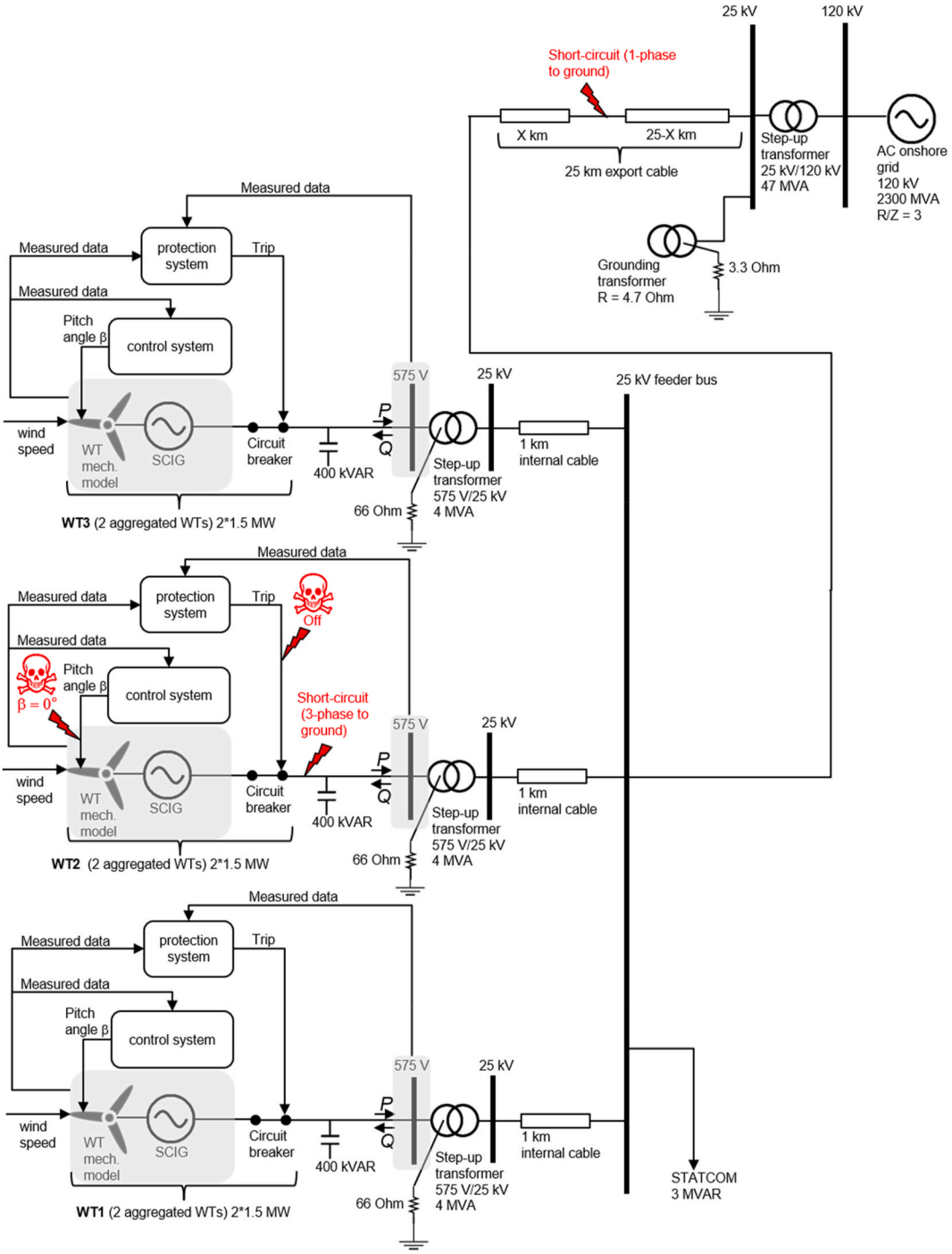

Fig. 2. Multi-domain simulation model of an OWF with AC export cable and individual wind turbines. Two manipulated quantities at Wind Turbine 2 (WT2) are shown: value of the pitch angle β and the Trip signal. Applied faults are also depicted: a short circuit at varying locations at the export cable and a short circuit at the terminals of WT2.

parameter is not needed, therefore the OWF is considered as a system with lumped parameters, described by ordinary differential equations (ODEs) (Rolf, 2007). Accordingly, there is no spatial (geometry) modelling and no spatial discretization, typical for the numerical simulation methods of systems with distributed (spatially dependent) parameters with partial differential equations, e.g. in (AiLong et al., 107350), (Ai et al., 2020). The action of the physical components is expressed through balance and constitutive equations. The connection between these components is expressed through node and mesh equations.

Our simulations employ the phasor solution method. The method is widely used to study the stability of multi-machine power systems, which consist of large generators and motors. However, it can be applied to any linear system and not only to such stability studies.

In the phasor solution method, the circuit differential equations are replaced by a set of algebraic equations evaluated at a fixed frequency, i.e. the fundamental frequency of the AC power system, in which the sinusoidal voltages and currents are represented as phasors. In our simulations a continuous phasor solver is used, which utilizes a full set of machine differential equations for modelling stator and rotor transients. In this way the electromechanical transients of the interaction between electrical, mechanical and corresponding control components, i.e. turbines, generators and respective controllers, are captured disregarding the very fast electromagnetical transients of the interaction between the purely electrical components, i.e. resistive, inductive and capacitive network elements. The electromechanical transients are the most important transients regarding major disturbances of the power system (Elgerd, 1982), as the ones investigated here, and the stability of the power system is mainly related to the electromechanical phenomena causing these transients (Machowski et al., 2011) compared to the electromagnetic and the thermal phenomena. The advantage of the phasor method is a dramatically reduced computational time.

The continuous phasor solution utilizes a variable-step ODE solver. We use the recommended Simulink solver (MathWorksa), (MathWorksb) with the ode23tb integration algorithm with a maximum time step of one cycle of the fundamental frequency. Accordingly, the maximal time step in our simulations is set to 1/60 s due to the fundamental frequency of 60 Hz of the models. The ode23tb solver computes the model's state at the next time step using a multistep implicit Runge-Kutta formula with a trapezoidal rule first stage, and a second stage consisting of a backward differentiation formula of order two (MathWorksc). The same iteration matrix is used in evaluating both stages.

Fig. 2 depicts the multi-domain large-scale OWF model with AC export cable and individual WTs. The model contains the models of 3 individual WTs with SCIGs, each driven by a variable-pitch fixed-speed wind turbine. The mechanical WT model aggregates two 1.5 MW turbines. The SCIG stator is connected to an offshore step-up transformer through which the low voltage level at the WT of 575 V is increased to the medium voltage level within the OWF of 25 kV. The active power P generated by the WT flows toward the export cable, while the reactive power Q flows in the opposite direction. Capacitor banks with 400 kVAR are connected at the low voltage bus of 575 V of each wind turbine in order to compensate partly the reactive power absorbed by the SCIGs. Internal AC cables, each with a length of 1 km, connect the transformers to the feeder bus collecting the power generated by all WTs. The OWF has a 3 MVAR static compensator (STATCOM) device also connected at the feeder bus. An AC export cable of 25 km length connects the feeder bus to the onshore step-up transformer at which the voltage is increased to the 120 kV level of the onshore grid. The onshore grid is modelled through an equivalent system with 120 kV and 2300 MVA.

Each of the individual WTs possesses an individual control and protection system. The STATCOM device has its own control system. The measured value of the generated electric output power is the dynamic input to the WT control system modelled as a proportional-integral (PI) controller. This value is compared to the rated mechanical power and the pitch angle is adjusted accordingly by the controller – constant at zero degrees when the measured electric output power is under the rated power value and increasing to keep the electric output power at the rated power value when this value is surpassed. By this adjustment, the rotor speed is kept practically constant at the value (1 pu) corresponding to the rated power (allowing 5% overspeed and no underspeed as normal operating conditions in this model according to the protection settings in Table. A.1 in the Appendix). This means, however, that the same mechanism is used for the control of the extraction of mechanical power from wind and the control of electrical power generation, which can facilitate the occurrence of abnormal values of the electrical quantities and the generated power by abnormal operation of the control system, e.g. the pitch angle manipulations considered here. Besides the operation of the WT according to the above presented control law the control system also counteracts disturbances.

Measured values of AC voltages and currents at the 575 V bus and of the rotor speed are inputs to the WT protection system for monitoring. When the measured values exceed their limit values for a longer interval than allowed a trip ("Trip") signal is sent by the protection system to the circuit-breaker. The signal opens the circuit-breaker (shown closed in Fig. 2) and the WT gets disconnected from the OWF grid. The limit values of the monitored quantities are given in Table. A.1 as settings for the protection system including the corresponding values of the intervals of allowed violation.

The results of the simulation are electrical quantities, i.e. active and reactive power, and mechanical quantities, i.e. pitch angle and rotor speed, of the WTs alongside with electrical quantities, i.e. currents and voltages, at the 25 kV feeder bus. The wind speed value is an input to the model.

Fig. 2 depicts the manipulated quantities for the simulation of the impact of cyber-attacks, i.e. pitch angle value β and trip signal of WT2, alongside with the two electrical faults applied at the model – a single-phase to ground short circuit at the export cable, and a 3-phase short circuit at the terminals of WT2. The manipulation of the pitch angle value means an imposition of a value $\beta = 0^\circ$ at a given time. The manipulation of the trip signal is modelled as a temporary deactivation of the protection system by delaying the generation of the signal by the protection system. Accordingly, following two scenarios were modelled and simulated: (1) imposition of $\beta = 0^\circ$ simultaneously with protection system deactivation for 100 s - as discussed in Kulev et al. (2019), and (2) imposition of $\beta = 0^\circ$ for 100 s. A constant wind speed of 15 m/s is used for the simulations, which corresponds to the rated (maximum) power and normal operating conditions.

The single-phase to ground short circuit was applied at varying locations at the export cable, which is presented by the distance X in km of the fault location to the feeder bus. Three locations were chosen corresponding to three values of X – 0.1 km 12.5 km 24.9 km. In this way, the fault is located at the midpoint of the cable and 0.1 km away from each end of the cable. This distance of 0.1 km corresponds to 1% of the characteristic cable length scale of 10 km in this case. Please note, the whole cable length is 25 km, i.e. 2.5 times the characteristic length scale of 10 km. Besides the variation of the fault location, the fault duration t_d was varied as well. Following five values were chosen for t_d: 0.005 s, 0.01 s, 0.05, 0.1 s and 0.185 s, based on preliminary explorations of the system response to disturbances.

The 3-phase short-circuit was applied at the terminals of WT 2, i.e. at the low voltage connection between the generator (SCIG) and the step-up transformer. In this way, the location of the fault was fixed. The duration of the fault was varied with a step of 0.001 s in order to determine the critical duration by which the WT, more specific the generator, is disconnected from the OWF. As mentioned before, this disconnection results from the opening of the circuit-breaker by the WT protection system with a trip signal.

Fig. 3 depicts a multi-domain large-scale OWF model with AC export cable, which uses six DFIG WT with 1.5 MW that are aggregated into a single WT (shown on the left). The DFIG consists of a wound rotor

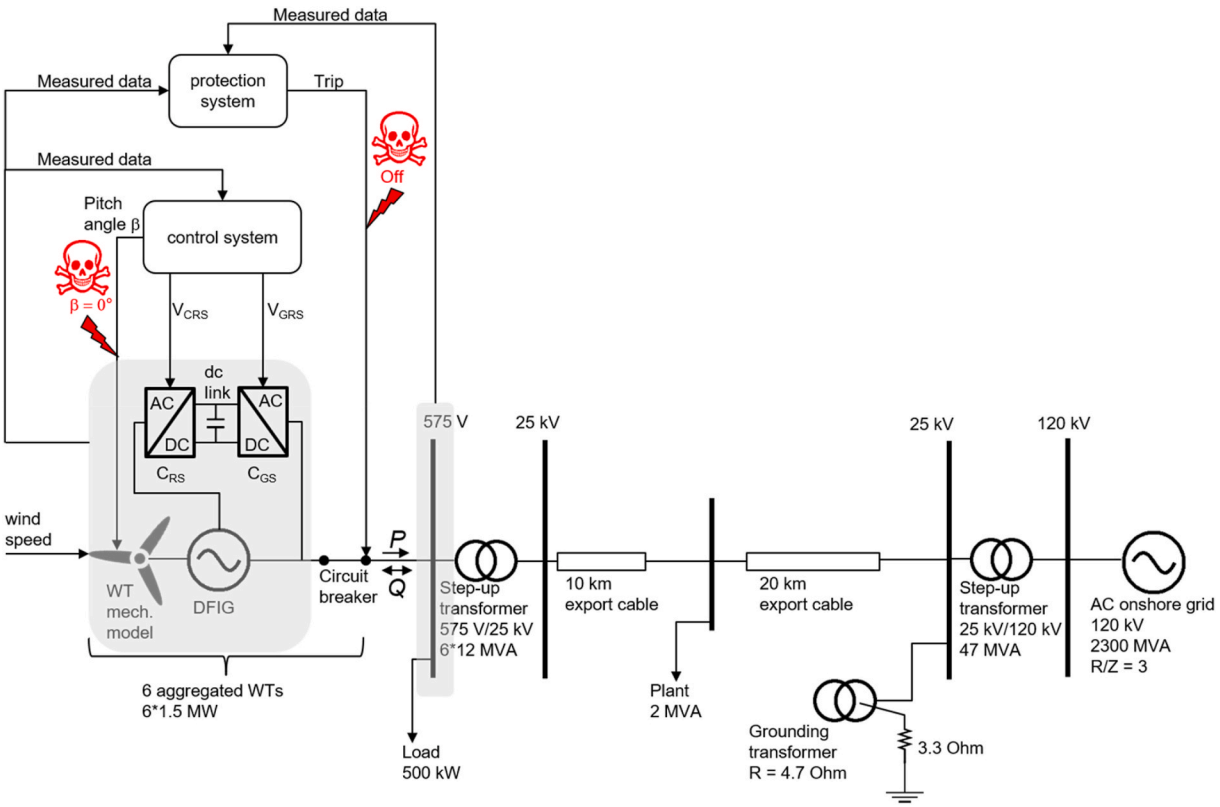

Fig. 3. Multi-domain simulation model of an OWF with an AC export cable and aggregated wind turbines. Two manipulated quantities are shown: pitch angle value and the Trip signal.

induction generator and an AC/DC/AC IGBT-based converter. The generator rotor is driven by a variable-pitch variable-speed wind turbine. The converter consists of two components, the rotor-side converter (C_{RS}) and the grid-side converter (C_{GS}), connected with a DC link. Both C_{RS} and C_{GS} use power electronic devices (IGBTs) to synthesize an AC voltage from a DC voltage source. The capacitor connected on the DC link acts as the DC voltage source. The stator is connected directly to the OWF grid whereas the rotor is connected through the AC/DC/AC converter to the OWF grid. The presence of power electronic converter allows the generation as well as the absorption of reactive power Q (indicated as bidirectional arrow). The generated electrical power P is transmitted by both the stator and the rotor windings to the low voltage bus of 575 V of the offshore step-up transformer, at which bus a load of 500 kW is connected as well. After raising the voltage to the 25 kV level, the electrical power is transmitted via a 30 km long AC export cable to the onshore step transformer.

Additionally, a 2 MVA plant is connected on the export cable. Before the generated power P is fed into the onshore AC grid, the voltage is raised to the 120 kV level of that AC grid by the onshore step-up transformer. The onshore AC grid is modelled through an equivalent system with 120 kV and 2300 MVA.

The model has a control system and a protection system, which enable the operation of the aggregated WT using measured data as input. The control system generates the control signal for the pitch angle β and the voltage control signals V_{RS} and V_{GS} for C_{RS} and C_{GS}, respectively. Like in the SCIG case, the control system has the tasks to counteract disturbances and to ensure energy conversion and generation according to a control law in dependence on the wind speed and the control strategy. This control strategy can be voltage reference value regulation or reactive power value regulation.

The pitch angle β is kept constant at 0° by low wind speeds until the measured rotor speed reaches ω_{rt}, which is the value of the rated WT mechanical power. Beyond ω_{rt}, the pitch angle is increased proportionally to the rotor speed deviation from ω_{rt} to limit the extracted WT mechanical power at its rated value by high wind speeds.

The control system uses the rotor-side converter C_{RS} through V_{RS} to control the WT active power and the voltage or reactive power measured at the WT terminals through measured values of power, AC currents and voltages, and the rotor speed. The active power is controlled to follow a pre-defined dependence on the rotor speed. The voltage or the reactive power at the grid terminals is controlled by the reactive current flowing in the converter C_{RS}.

Thus, two different but interrelated mechanisms are used for the control of mechanical power extraction and the control of electrical power generation. In this way an abnormal operation of the mechanical power control, e.g. the manipulations of the pitch angle, would have a less pronounced or different effect on the electrical quantities and power than by the SCIG.

The control system uses the converter C_{GS} through V_{GS} to control the voltage of the DC link capacitor using measurements of AC currents and of the DC voltage.

The protection system of the DFIG WT acts in the same way as the above-mentioned protection system of the SCIG WT. The same measured AC voltages and currents at the 575 V bus alongside with the rotor speed are also monitored by the DFIG protection system. For the AC voltages and currents the same settings of limit values and intervals are valid, as seen in the DFIG row in Table. A.1. The only additional monitored electrical quantity is the DC voltage of the DC link. In contrast to the SCIG WT the DFIG WT has a much wider operational range of the rotor speed allowing 70% underspeed and 50% overspeed around the value of 1 pu.

Fig. 3 depicts the manipulated quantities for the simulation of the impact of cyber-attacks – pitch angle value β and trip signal of the aggregated WT. Thus, the manipulation is identical to the above-mentioned manipulation of WT2 and the description of the manipulation is valid here, too. Again, two scenarios were modelled and

simulated: (1) imposition of $\beta = 0^\circ$ simultaneously with protection system deactivation for 100 s, as discussed in Kulev et al. (2019), and (2) imposition of $\beta = 0^\circ$ for 100 s. A constant wind speed of 20 m/s is used for the simulations, which corresponds to the rated maximum power and normal operating conditions.

3.2. Disturbance impact index

As discussed in (Preda, 2016), the transient behavior of a power system due to a disturbance is determined by the disturbance characteristics and by the electrical distance between the location at which the disturbance occurred and the affected element, e.g. generator, load, or line. Accordingly, a formalized quantification of the disturbance impact is given by the so-called disturbance impact index (DII). A generic form of the DII reads (Eremia and Shahidehpou, 2013):

$$DII = f(k, x_d) \tag{1}$$

where k expresses the electrical distance between the disturbance point and disturbance impact, and x_d represents the disturbance characteristics, e.g. magnitude and duration. In this manner, the DII relates the disturbance characteristics to the disturbance impact. DII can also be understood as a measure for the system sensitivity to the disturbance characteristics and for the disturbance propagation.

A specific form of the DII regarding the disturbance impact on generators performance results from (Eremia and Shahidehpou, 2013), (Preda, 2016):

$$DII = \frac{Yt_d^2 \Delta P(Y, t_d)}{2H} \tag{2}$$

where the measure of the electrical distance to the disturbance point is given by the magnitude of transfer admittance Y, t_d means the disturbance duration, ΔP is the maximal deviation of the active power of the generator from the pre-disturbance value and H is the inertia constant of the generator. ΔP depends on both Y and t_d, also indicated by the results presented in Section 4.2.1. The system performance impairment is given as an absolute measure using ΔP.

4. Results and discussion

This section presents and discusses the obtained results.

4.1. Disturbances due to a cyber-attack

Both the OWF model with individual WTs (see Fig. 2) and the aggregated OWF model (see Fig. 3) were employed for the simulation of the manipulation of the WT control and protection systems according to the above-mentioned scenario discussed in Kulev et al. (2019). Thus, the simulations deliver explicit quantifications of the impact of the manipulation. Furthermore, they represent the system sensitivity to the fault in quantitative terms – as a dependence of the system response on the manipulation duration and in relation to the critical values of relevant quantities that lead to damages or service interruption. The simulations provide also the time scales of the transient behavior in response to the manipulation and of the propagation of disturbance from one domain (control, protection) into another (electrical, mechanical). The obtained results are relevant for real OWF, having in mind that WT tower collapse due to rotor overspeed and WT fire incidents due to overheating have been experienced on multiple occasions (Garcia-Sanz and Houpis, 2012).

4.1.1. OWF model with individual WTs

The first scenario represents a manipulation of the control and the protection system, as shown in Fig. 2, (Kulev et al., 2019). Fig. 4 depicts the initial steady-state of the system, established by a value of the pitch angle to 22.6 deg (see curve "pitch angle (deg)), and the resulting transient curves from the manipulation. A step change of the pitch angle to 0 deg is imposed at $t = 80$ s. The direct consequence of the manipulation is the immediate increase of the rotor speed of WT2 ("rotor speed (pu)). As a consequence of the rotor speed deviation the generated power ("Generated power (MW)") first peaks to almost 6 MW (twice the rated power of 3 MW prior to the manipulation) within 0.24 s after the manipulation, then drops beneath zero within 1.6 s and remains negative throughout the manipulation. Simultaneously, the reactive power ("Reactive power (Mvar)") at WT2 peaks to more than 6.74 Mvar, which corresponds to more than 4.5 times of the pre-manipulation level, and remains abnormally high with nearly factor 3 of the pre-manipulation level. Accordingly, only 5.47 s after the start of the manipulation WT1 and WT3 get tripped by their protection systems due to an AC undervoltage provoked by the drastically abnormal values of the electrical quantities at WT2 caused by the manipulation. Accordingly, both the generated power ("Generated power (MW)") and reactive power ("Generated reactive power Q″) at WT1 and WT3 become zero after 5.49 s the start of the manipulation. By that time all WT have practically stopped to generate power, and thus, the service of the whole OWF is interrupted!

Due to the electrical connection between the WTs within the OWF, the deviations of the electrical quantities at one system element, in this case WT2, propagate to the other system elements, here WT1 and WT3, and affect them as well. This illustrates the so-called hidden interactions between the system elements that are manifested under disturbed operating conditions as discussed in (Kröger and Zio, 2011).

Within 30 s after the start of the manipulation, the rotor speed of WT2 reaches an extreme overspeed value which is more than 2.5 times the nominal value which is observed longer than the allowed interval (see Table. A.1). Such a sustained overspeed poses clearly a danger of severe structural and component damage or destruction.

At $t = 180$ s, WT2 gets tripped both due to AC overcurrent and rotor overspeed. After the tripping of WT1 and WT3 at $t = 85.47$ s, their pitch angles are decreased to 0° in a predefined manner associated with overspeed values which the model foresees after tripping.

A variation of this scenario was simulated by which only the pitch angle of WT2 was manipulated by setting $\beta = 0^\circ$ at 80 s as shown in Fig. 3 and the protection system of WT2 was switched on (not manipulated). The results are shown in Fig. A.1 in the Appendix. Only 0.54 s after the start of the manipulation, WT2 is tripped by its protection systems due to AC undervoltage resulting from the continuous drop of the generated power. Again, within 30 s after the start of the manipulation, an extreme rotor overspeed of WT2 is reached and sustained throughout the duration of the manipulation.

The other two turbines WT1 and WT3 continue to work without interruptions due the severe deviations of the generated and reactive power of WT2 and its tripping. That means, after damped oscillations of their generated and reactive power the pre-manipulation values are practically restored within 4 s after the start of the manipulation.

The results of both simulations show that the severity of the manipulation impact - on the directly affected WT and on the other WTs as well - depends on the extent of the manipulation, i.e. only the control system or both the control and protection system are manipulated. One should note that in both cases there is a provoked interruption of service under otherwise normal operating conditions which besides the manipulation cannot cause interruption, i.e. lack of grid faults and wind speeds under the cut off values.

4.1.2. OWF with aggregated WTs

The same two procedures were applied for the modelling and simulation of the scenario described in Kulev et al. (2019) using the model shown in Fig. 3 as well. In the first case, depicted in Fig. 5, the manipulation of the pitch angle starts at $t = 80$ s with a step change of its initial steady-state value of 18.9° by imposing a value of 0° (see curve for "pitch angle (deg)" in Fig. 5). Simultaneously, the protection system is kept disabled until t = 180 s. The manipulations of both systems are then

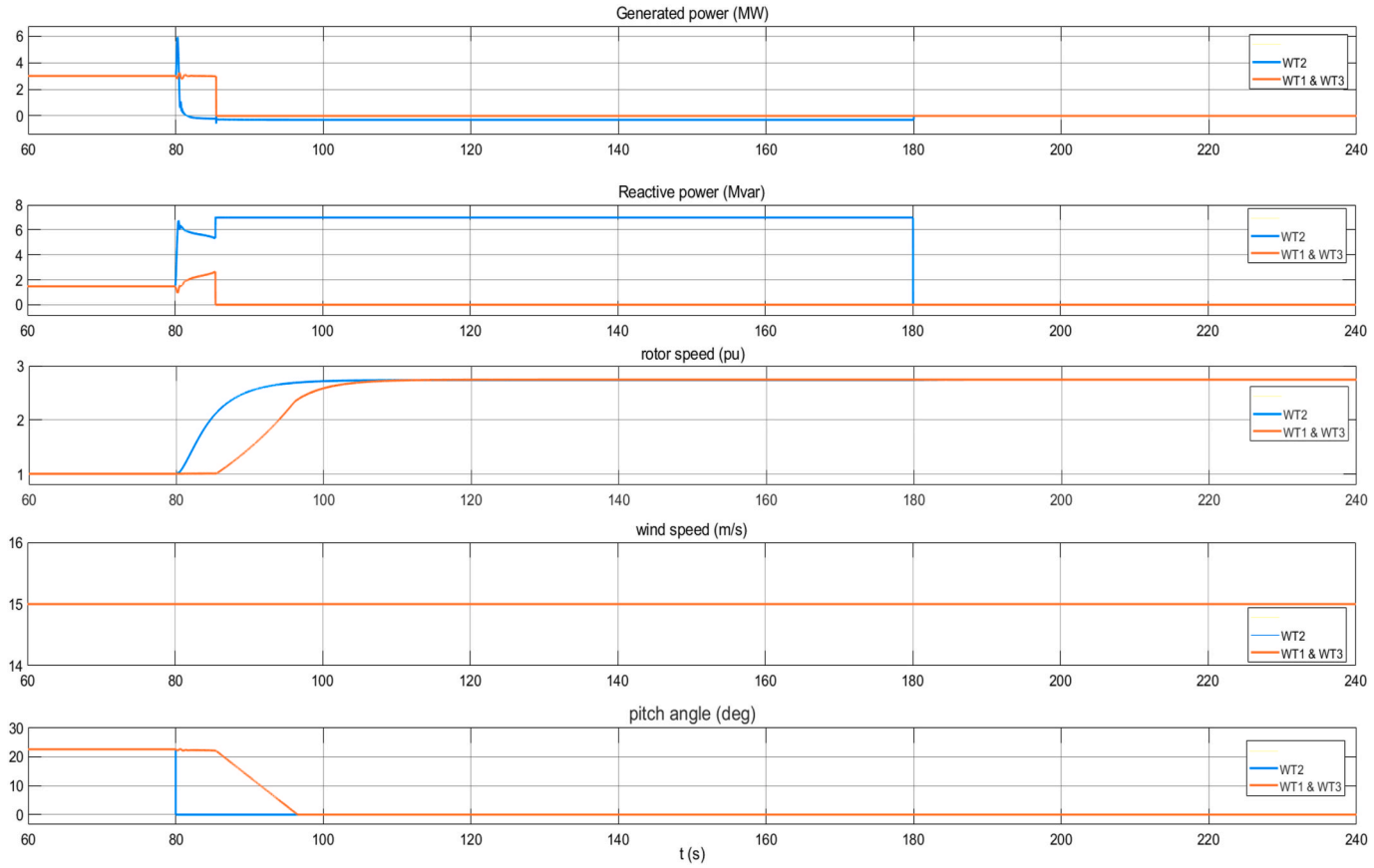

Fig. 4. Time evolutions of the electrical and mechanical quantities at the individual WTs (WT1 to WT3) before, during and after the manipulation of the pitch angle at WT 2 with manipulation of its protection system by delaying its action until the end of the manipulation at $t = 180$ s.

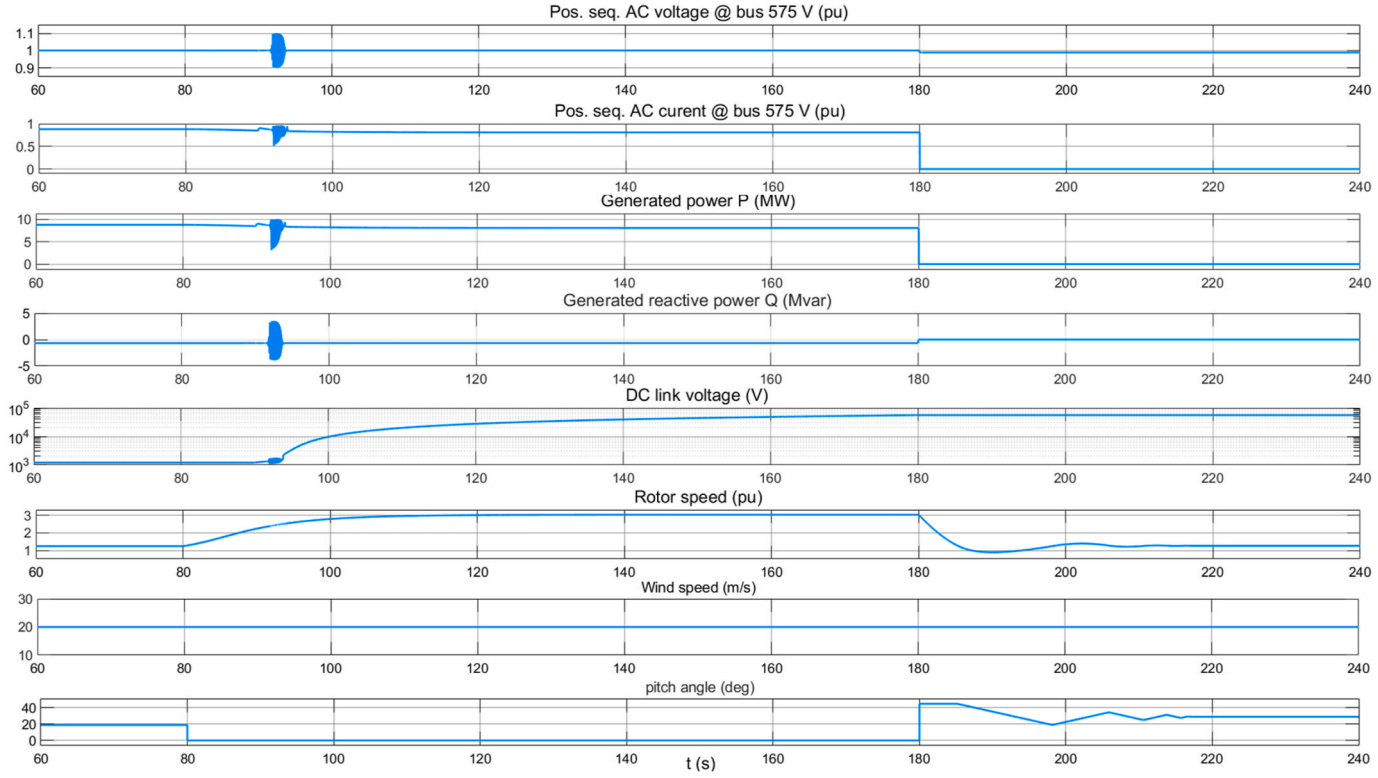

Fig. 5. Time evolutions of the electrical and mechanical quantities at the aggregated WT before, during and after the manipulation of the pitch angle with manipulation of the protection system by delaying its action until the end of the manipulation at $t = 180$ s.

removed at 180 s.

After the start of the manipulation, the rotor speed ("Rotor speed" in Fig. 5) starts to increase. At around $t = 91$ s, abnormal oscillations of the electrical variables occur, which are eventually damped out by the control system. An uncontrolled increase of the DC link voltage ("DC link voltage" in Fig. 5) starting after the end of the oscillations can be observed.

A sustained steady-state rotor overspeed of more than twice the maximal allowed rotor velocity, is reached within 40 s after the start of the manipulation. It would lead to a mechanical overload causing a structural damage of the WT or a collapse of the WT tower, e.g. as reported in (Garcia-Sanz and Houpis, 2012).

Besides the rotor overspeed, one can observe in this case a sustained and increasing excessive DC overvoltage which is only allowed for 0.001 s, according to the protection system settings in Table. A.1. Around 30 s after the start of the manipulation, the DC voltage is 10 times higher than the maximal allowed value. The thermal time constants of semiconductor components - like the IGBT devices on both sides of the DC link are very short - hundreds of milliseconds or seconds, depending on size and design (Ackermann, 2012). Doubtlessly, this would lead to overheating resulting into a fire threat, similar to the WT fire incident reported in (Garcia-Sanz and Houpis, 2012), by DC link voltages as by the manipulation simulations.

The WT is tripped at $t = 180$ s, when the protection system is activated, both due to rotor overspeed and DC overvoltage. The control system restores the nominal rotor speed after the manipulation by an adjustment of the pitch angle. However, at that time the DC link voltage ("DC link voltage" in Fig. 5) is more than 20 times higher than the allowed maximum value. The model does not include a reconnection after the tripping, and thus, the WT remains disconnected after the manipulation.

In the second simulation, depicted in Fig. A.2 in the Appendix, the manipulation starts at $t = 80$ s by setting the pitch angle to 0° which is removed at $t = 180$ s. The protection system is not disabled. After the start of the manipulation, the rotor speed ("Rotor speed") starts to increase while the DC link voltage ("DC link voltage") exhibits a jump that is counteracted by the control system. At $t = 88$ s, the WT is disconnected due to rotor overspeed by the protection system via activation of the circuit breaker. In this way, the manipulation causes an interruption of service due to the disconnection. The voltage at this bus ("Pos. seq. AC current @ bus 575 V″) remains practically the same.

Again, the rotor speed reaches a steady-state value twice the maximum allowed value of 1.5 pu (see Table. A.1) during the manipulation within 40 s. After the end of the manipulation, the control system restores the nominal speed of the rotor by adjusting the value of the pitch angle. Again, the WT remains disconnected after the manipulation.

It should be emphasized that the above mentioned excessive overspeed, leading to mechanical overloads capable of causing structural damages or a collapse of the WT tower, is the result of the manipulation of just a single operational parameter, i.e. the pitch angle, which makes it less detectable that the first case. In contrast, the first case requires the manipulation of the pitch angle as well as the deactivation of the protection system, which increases the level of needed effort and of detectability. However, given the exponential increase of the DC link voltage and the fact that the maximum voltage value can be exceeded only for 0.001 s the first case might have much more drastic consequences.

4.2. Short-circuit faults

Short-circuit faults are, beside cyber-attacks, a constant threat for the operability of OWF. This kind of faults can be provoked by natural causes, e.g. by sediment scour (Jones et al., 2018), accidently by lowered anchors (Carbon Trust, 2015) or even maliciously intended (Sill Torres et al., 1109). Motivated by this observation, the impact of such faults has been studied using the models introduced in Section 3.

4.2.1. Short-circuit single-phase fault at the export cable

The OWF model depicted in Fig. 2 was used for the investigation of the single phase to ground short-circuit at the export cable. A variation of the short-circuit location and duration was performed as described in Section 3.1. The goal was to produce simulation results that represent the sensitivity of the system response to this variation, and thus, to determine the critical values of the fault duration leading to interruption of service. Related to this, the DII was applied for the assessment of the mentioned sensitivity, regarded as safety-level index, too. The results are relevant for the design of OWF control and protection systems with their settings regarding faults due to ship anchor incidents.

The typical disturbance behavior of the OWF is presented through selected time evolutions of the generated active power of all three WTs – prior, during and after the disturbance, applied at $t = 15$ s. The results are depicted in Fig. 6 and in Figs. A.3-A.4 in the Appendix. Since the distance from the fault location to each WT is the same, the evolution curves corresponding to each WT are identical and therefore only curve can be seen on each figure. The time evolutions are typically damped oscillations. The critical duration of $t_{d,cr} = 0.186$ s is independent of the fault location. By this duration, critical values of the AC voltages at the WT are exceeded for a longer period than allowed (see Table. A.1) and the WTs are disconnected by their protection systems. Please note, that is not shown in the figures.

The simulations indicate the dependence of the deviation of the generated power of the WTs from its duration t_d and its undisturbed value on the geometric distance to the disturbance. The latter is equal to the sum of the length of export cable portion corresponding to the disturbance location and the length of the internal cable. Comparing Fig. 6 to Fig. A.3, one can note that a longer distance leads to a greater deviation, which is non-trivial. On the other side, the results in Fig. 6 and Fig. A.4 indicate that the longer the duration the greater the deviation.

The values of the *DII* with the variation of the disturbance distance and duration t_d are presented in Fig. 7 for a single WT. Since both the geometrical and electrical distance between disturbance and each individual WT is the same, the DII values are identical for all WTs.

The functional dependence of the *DII* on both the disturbance duration and distance is non-linear and monotonically increasing.

The values of the *DII* express quantitively the sensitivity of the system performance impairment, i.e. the deviation from the undisturbed value, to the variation of these characteristics. A zero value would correspond to lack of system performance impairment, and therefore, can be regarded as the highest level of operational safety. The increase of the DII values would correspond to a decrease of the level of operational safety, accordingly. The highest value – right before tripping – corresponds to the lowest level of safety because practically any additional disturbance would lead to interruption of service. Thus, broadly speaking, the values of the *DII* curves give the level of the operational (un-)safety of the system regarding the above-mentioned disturbances with their specific characteristics. This means, what additional disturbance can be accommodated without interruption of service or how far is the system by the current disturbed conditions from this point.

On the other side the above results indicate that the same impact of a ship anchor on the export cable would cause a bigger absolute performance impairment (given by ΔP) through such a short-circuit if the ship is the more distant from the OWF WTs, which is as already mentioned non-trivial.

4.2.2. Short-circuit three-phase fault at the terminals of a wind turbine

The OWF model in Fig. 3 was used for the investigation of the three-phase to ground short-circuit at the terminals of an individual Wind Turbine 2 (WT2), as explained in Section 3.1. The goal was to identify the critical value of this duration regarding the directly affected WT2. This included the investigation the fault influence on the other two WTs, in terms of fault propagation, since the internal OWF cable system of the model is AC system allowing internal electrical faults to propagate within it. The results are relevant, since the maintenance of the WTs

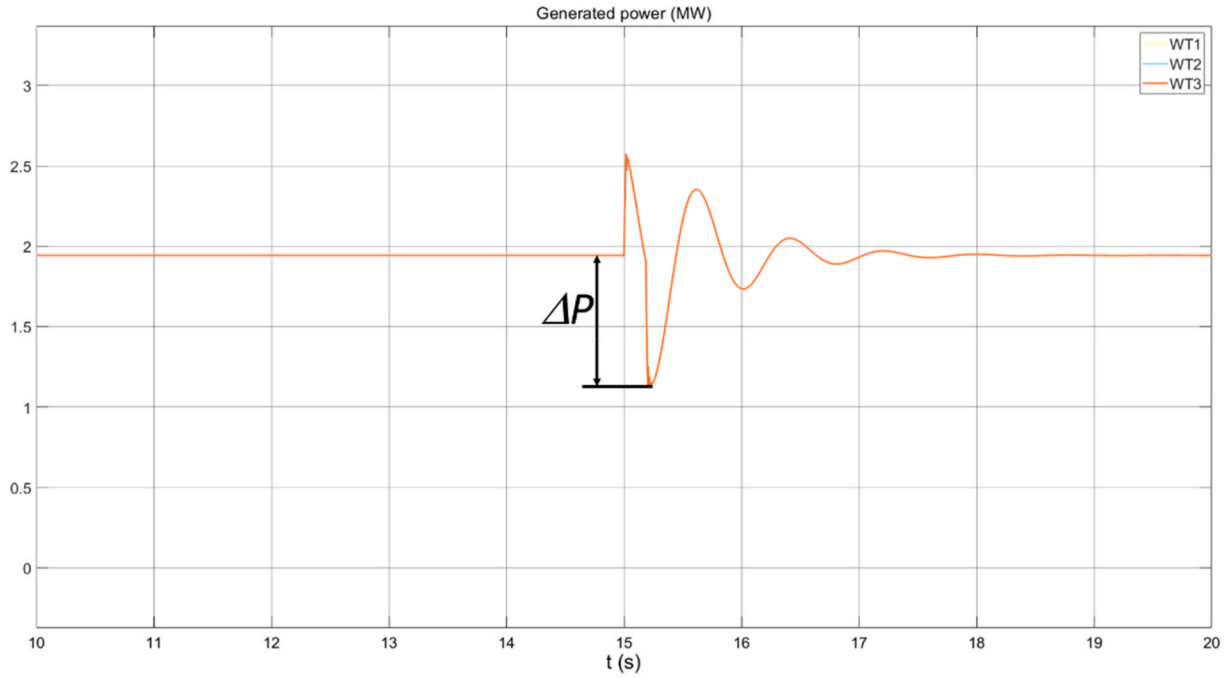

Fig. 6. Time evolution of the generated power at WT1 to WT3 for 25.9 km geometrical distance and disturbance duration $t_d = 0.185$ s ΔP indicates the maximal deviation of the active power of the generator.

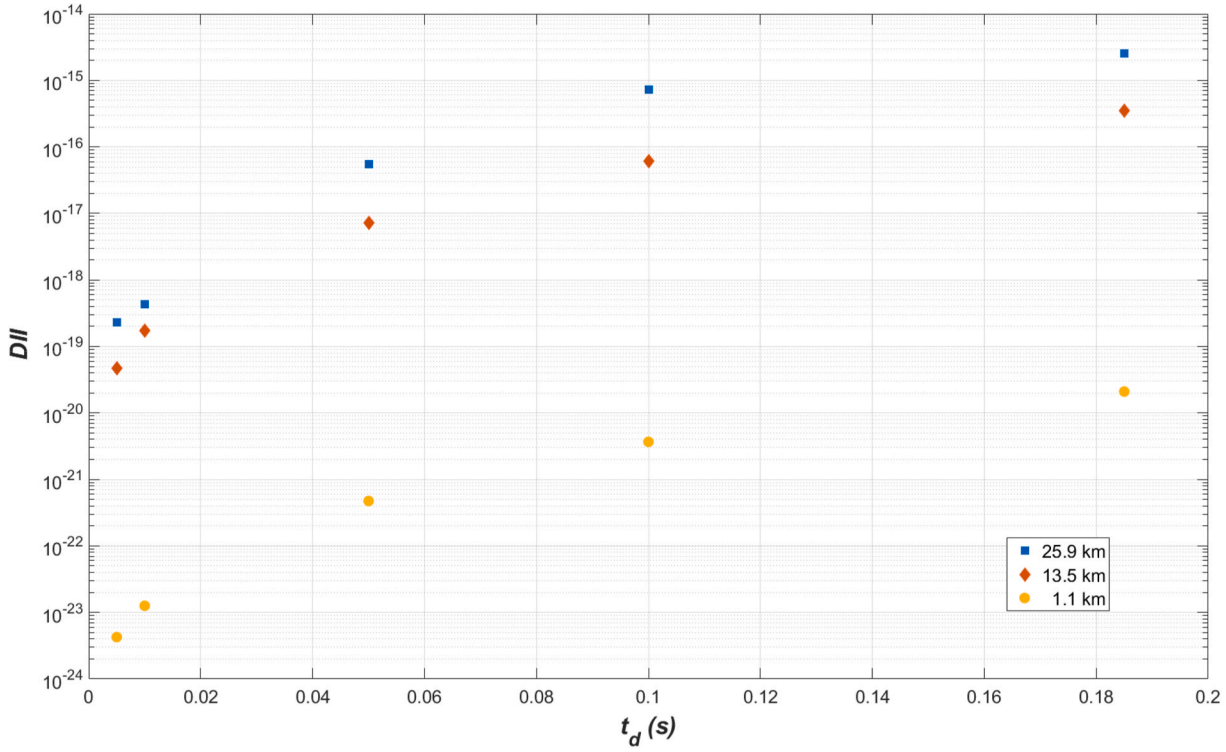

Fig. 7. Disturbance impact index (*DII*) with the variation of the disturbance distance and duration t_d.

requires a lot of vessels, which increases the likelihood of a vessel collision with a WT tower leading to such severe fault.

Time evolutions of the generated active power are shown in Figs. 8 to 9 for two critical values of the disturbance duration. The short circuit is applied at $t = 15$ s by a fully established steady state causing typical oscillatory time evolutions. A disturbance duration of $t_{d,cr1} = 0.091$ s leads to the tripping of WT 2, at which terminals the disturbance is applied, by its protection system at $t = 15.104$ s (see Fig. 8). In contrast, the control systems of WT1 and WT3 succeed to return both WTs to the undisturbed value after the initial dip due to the disturbance and the following oscillations. However, a disturbance duration of $t_{d,cr2} = 0.101$ s leads, after the tripping of WT2 (at $t = 15.104$ s), to the tripping of WT1 and WT3 by their protection systems (at $t = 15.11$ s), as shown in Fig. 9.

The results indicate that the fault at one OWF system element

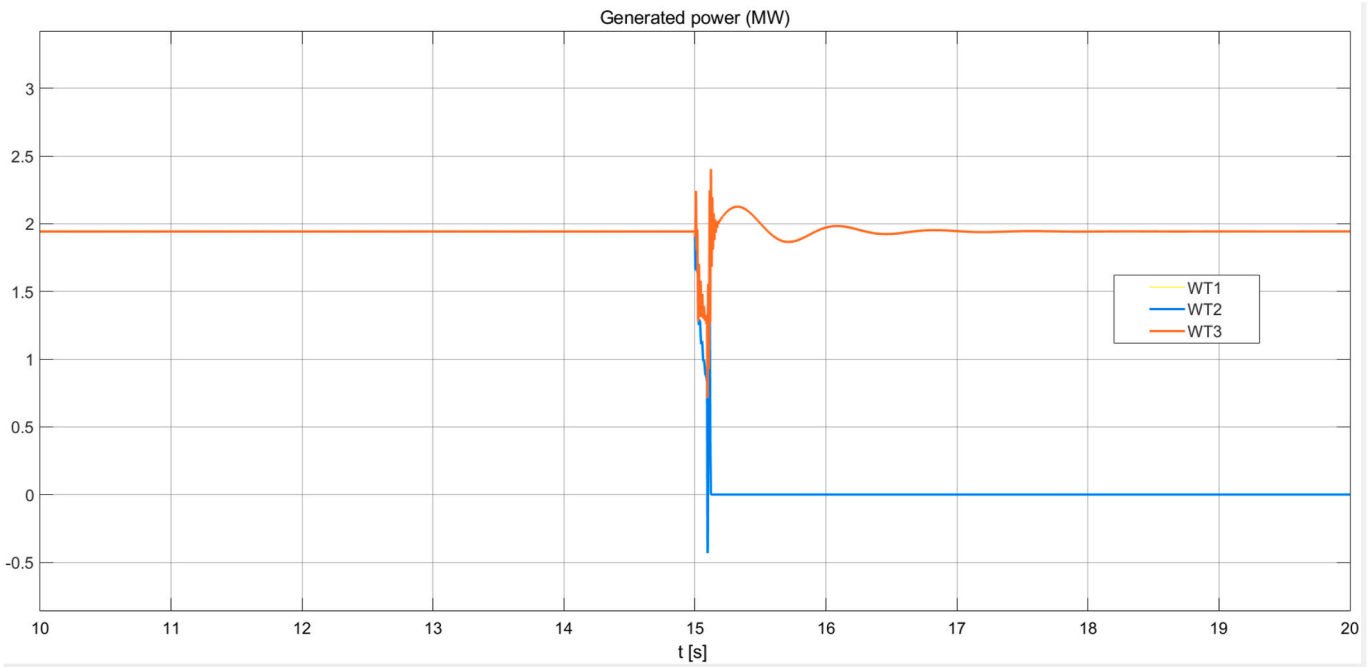

Fig. 8. Time evolution of the generated power through the WTs by the short circuit with a critical duration of $t_{d,cr1} = 0.091$ s.

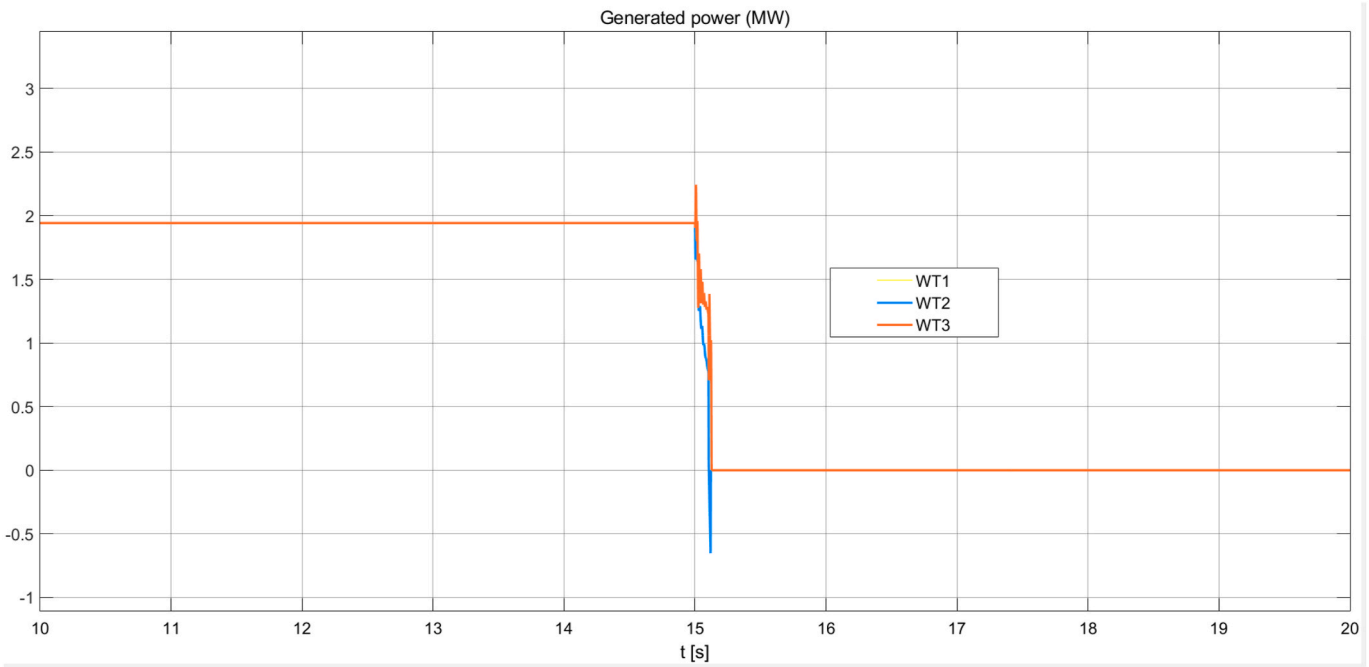

Fig. 9. Time evolution of the generated power through the WTs by the short circuit with a critical duration of $t_{d,cr2} = 0.101$ s.

propagates within the internal OWF AC grid influencing remaining system elements. Due to this propagation and depending on the fault duration besides the directly affected system element the remaining system elements get also affected as service interruption due to the above-mentioned tripping.

That means, a fault with a sufficient duration occurring at low-voltage terminals of one WT affects not only this WT, but propagates through the medium-voltage internal cable system and affects the remaining WTs. Because of this fault sensitivity and fault propagation within the OWF system, a hidden interaction among the WTs under normal operating conditions becomes evident by the disturbed conditions due the fault. It was pointed out in (Kröger and Zio, 2011) that such hidden interactions between the system elements might be crucial for the development of the cascading failure event.

5. Conclusions

The impact of the manipulation of the control and protection systems action due to cyber-attacks discussed in previous works was quantified and investigated through simulations. The simulations results give a quantitative confirmation of the qualitative conclusions from Kulev et al. (2019) regarding the mechanical quantities, i.e. rotor overspeed,

and delivers new results concerning electrical quantities at the WT, i.e. the outstandingly abnormal active and reactive power at the single SCIG WT with the resulting influence on the remaining SCIG WTs and the extreme DC link voltage at the aggregated DFIG WT. One can clearly state that an interruption of service of the OWF and single WTs is possible under normal operating conditions through such a manipulation. Furthermore, already the manipulation of individual WTs can lead to an interruption of service of the whole OWF - illustrating the exceptional severity of the disturbance impact of malicious intentional acts, the propagation of this impact within the OWF system and the sensitivity of the OWF elements to it. Additionally, the results clearly indicate that damages beyond the scope of the usual maintenance process are possible under normal operating and grid conditions due to the attacks.

A possible countermeasure against such attacks would be a Reference Technical Systems (RTS) (Kulev et al., 2019). Such an RTS would simulate in real time the system with a simplified model. Deviations between real and modelled behavior would indicate abnormal activities. The simulations above give both the typical, i.e. reference, behavior of the OWF by normal operating conditions and the estimated abnormal behavior of the real system due to the manipulations, i.e. the characteristic peak and fall of the SCIG power and the oscillations of the DFIG electrical quantitates. These characteristic deviations from normal behavior due to manipulation could serve exactly as a real time indicator of an ongoing attack.

An investigation of the impact of a short-circuit at the OWF export cable on the WTs was performed through simulations with varying fault location and duration. The dependence of the impact on the location and the duration was determined as well as the critical value of the fault duration leading to interruption service. The sensitivity of the impact to the location and duration was quantified and assessed through the disturbance impact index. Additionally, the impact of short-circuit at the terminals of a WT was performed through simulations by varying the fault duration. Results with a critical value of the fault duration leading to interruption service of the directly affected WT were presented. During the disturbed conditions, an interaction between the WTs appears due to the fault propagation and sensitivity within the AC part of the OWF. One should note that such interaction remains hidden by normal conditions.

As a principal contribution of this work the simulations indicate that sufficiently severe HILP disturbances, provoked by malicious acts or natural causes, at single WTs can affect the remaining WTs, and thus, lead to an interruption of the service of the complete OWF. The results confirm the possibility of such OWF system failure as in Hornsea1,[6] the lack of short-term resilience (Panteli and Mancarella, 2017) and of power system security (Kundur et al., 2004) of the OWF towards such events. The obtained results of this study provide valuable insights into the internal processes of the OWF energy system during such disturbances and the related vulnerabilities against such threats. Consequently, this outcome of this work supports future developments towards more secure and reliable OWF systems.

CRediT authorship contribution statement

Nikolai Kulev: Conceptualization, Methodology, Software, Investigation, Data curation, Writing – original draft, Visualization. **Frank Sill Torres:** Writing – review & editing, Supervision, Project administration, Funding acquisition.

Declaration of competing interest

The authors declare that they have no known competing financial interests or personal relationships that could have appeared to influence the work reported in this paper.

Appendix

Table A.1
Settings of the WT protection systems with the Squirrel-Cage Induction Generators (SCIG) for the individual WTs model and Doubly-Fed Induction Generators (DFIG) for the aggregated WTs model.

	SCIG	DFIG
Instantaneous AC Overcurrent	10 pu	10 pu
Positive-sequence AC Overcurrent/Interval	1.1 pu/10 s	1.1 pu/10 s
AC Current Unbalance/Interval	0.4 pu/0.2 s	0.4/0.2 s
Positive-sequence AC Undervoltage/Interval	0.75 pu/0.1 s	0.75 pu/0.1 s
Positive-sequence AC Overvoltage/Interval	1.1 pu/0.1 s	1.1 pu/0.1 s
Negative-sequence AC Voltage Unbalance/Interval	0.05 pu/0.2 s	0.05 pu/0.2 s
Zero-sequence AC Voltage Unbalance/Interval	0.05 pu/0.2 s	0.05 pu/0.2 s
DC link voltage/Interval	–	1900 pu/0.001 s
Rotor Underspeed/Interval	1 pu/5 s	0.3 pu/5 s
Rotor Overspeed/Interval	1.05 pu/5 s	1.5 pu/5 s

[6] https://www.theguardian.com/business/2019/aug/16/national-grid-blackout-report-avoidable-faults-blamed.

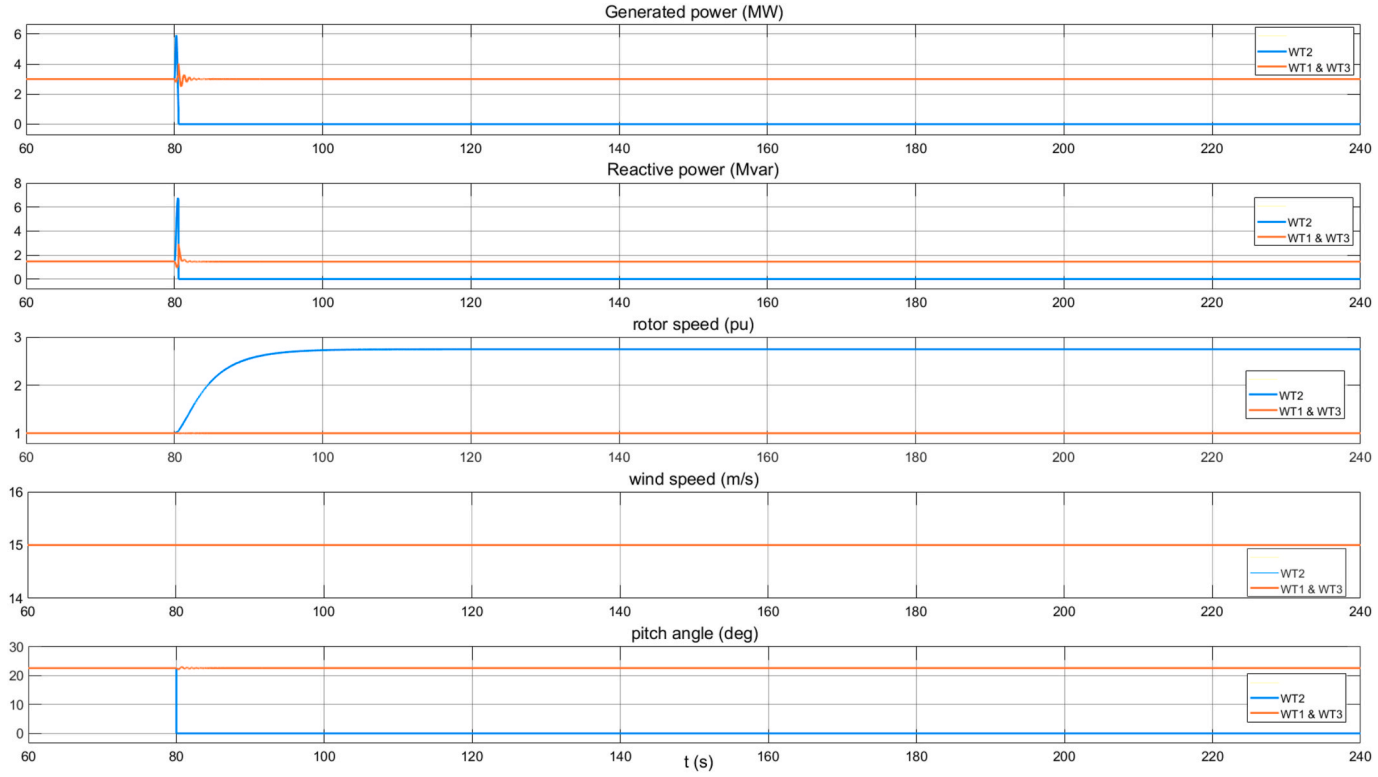

Fig. A.1. Time evolutions of the electrical and mechanical quantities at the individual WTs (WT1 to WT3) before, during and after the manipulation of the pitch angle at WT 2 without manipulation of the action of its protection system.

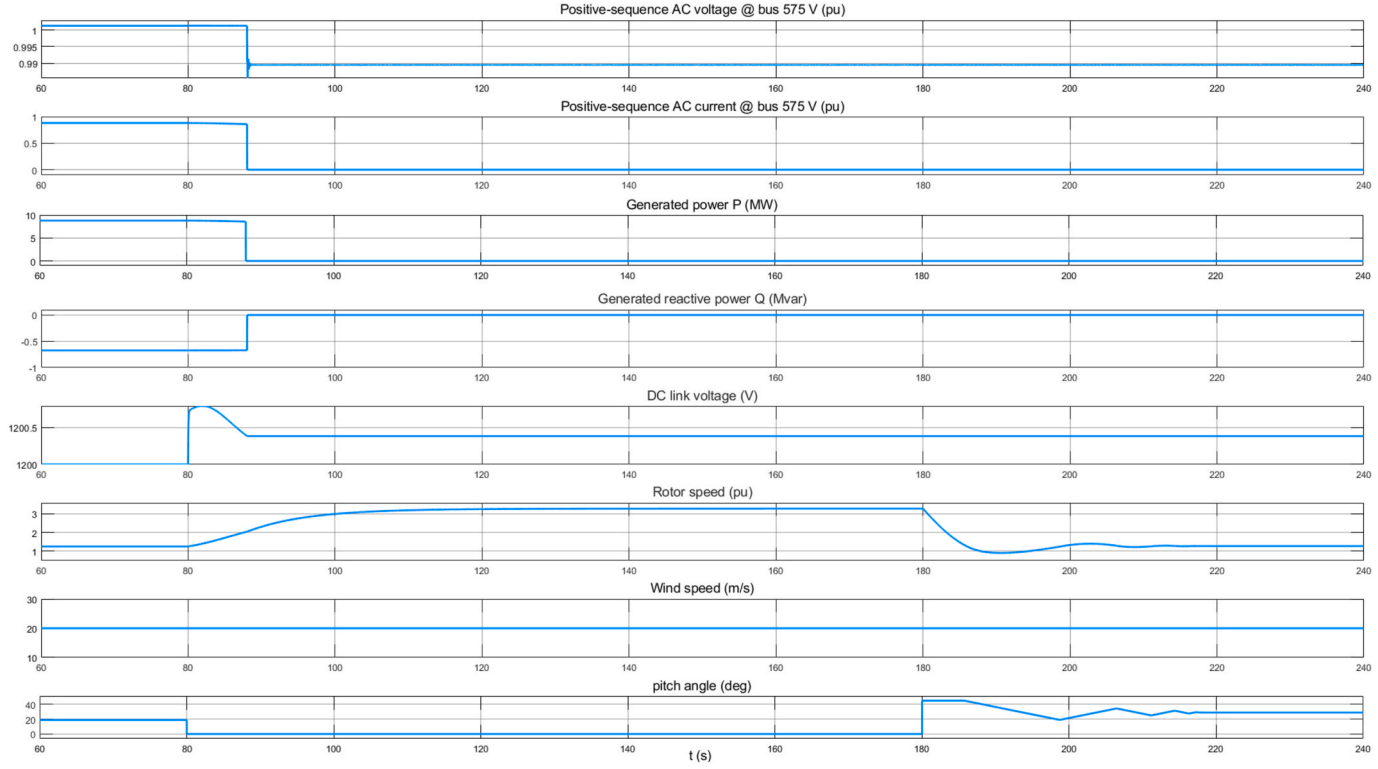

Fig. A.2. Time evolutions of the electrical and mechanical quantities at the aggregated WT before, during and after the manipulation of the pitch angle without manipulation of the action of the electrical protection system.

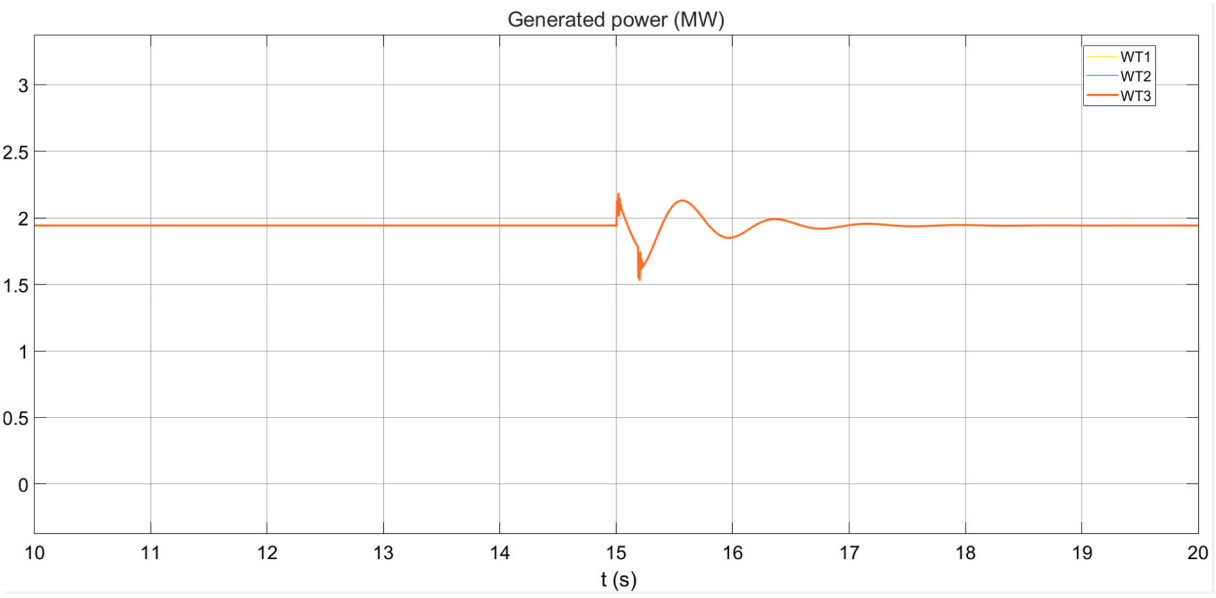

Fig. A.3. Time evolution of the generated power at WT1 to WT3 for 1.1 km geometrical distance to the disturbance and $t_d = 0.185$ s

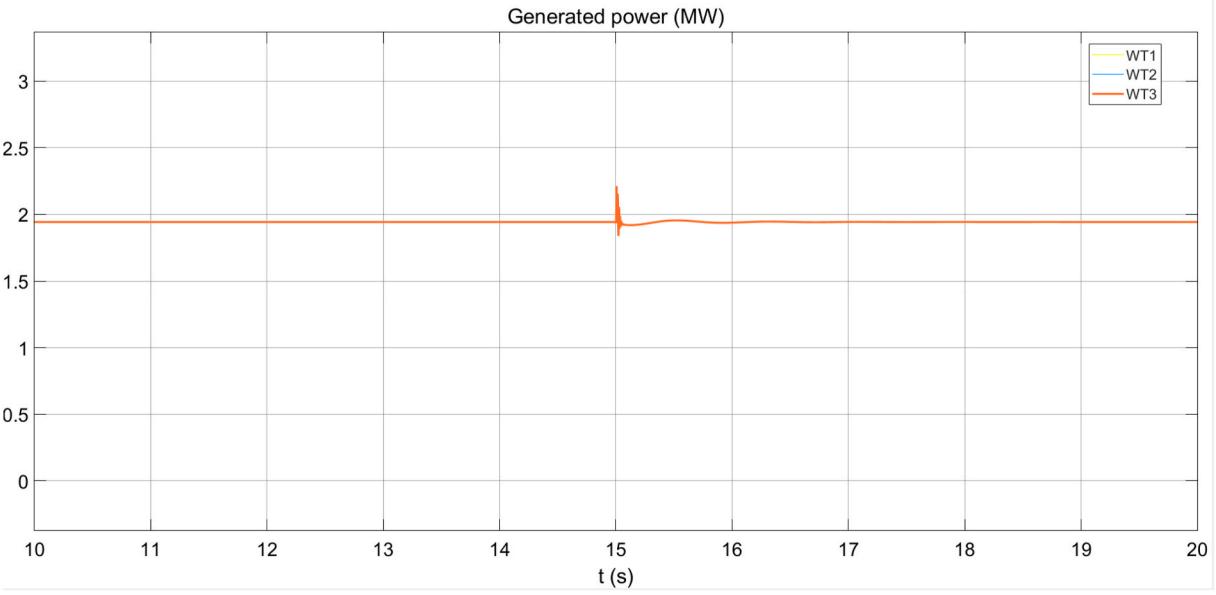

Fig. A.4. Time evolution of the generated power of the generated power at WT1 to WT3 for 25.9 km geometrical distance to the disturbance and $t_d = 0.005$ s

References

Ackermann, T. (Ed.), 2012. Wind Power in Power Systems". John Wiley & Sons Ltd, ISBN 978-0-470-97416-2.

Ahmed, M.A., Kim, C.-H., 2017. Communication architecture for grid integration of cyber physical wind energy systems. Appl. Sci. 7 (10), 1034. https://doi.org/10.3390/app7101034.

Ai, Yuewei, Liu, Xiaoying, Huang, Yi, Long, Yu, 2020. Numerical analysis of the influence of molten pool instability on the weld formation during the high speed fiber laser welding. Int. J. Heat Mass Tran. 160, 120103, 0017-9310.

Ai, Yuewei, Long, Yu, Huang, Yi, Liu, Xiaoying, 2022. The investigation of molten pool dynamic behaviors during the "∞" shaped oscillating laser welding of aluminum alloy". Int. J. Therm. Sci. 173 (2022). ISSN 1290-0729, 107350.

Anaya-Lara, O., Campos-Gaona, D., L Moreno-Goytia, E., Adam, G.P., 2014. Offshore Wind Energy Generation: Control, Protection, and Integration to Electrical Systems". John Wiley & Sons, Ltd., ISBN 978-1-118-53962-0

Arthur, Ekwue, Oona, Nanka-Bruce, Rao, Jhansi, Damien, McCool, 2008. Dynamic stability investigations of the fault ride-through capabilities of a wind farm. In: Proceedings of the 16th Power System.

Aven, T. (Ed.), 2018. Society for Risk Analysis Glossary".

Bolik, S.M., 2008. The Impact of Grid Codes on the Development of Wind Turbine Technologies", 7th International Workshop Large-Scale Integration Wind Power into Power System. Madrid, Spain.

Carbon Trust. Cable Burial Risk Assessment Methodology", vol. 835, 2015. CTC, UK.

Chou, C.J., Wu, Y.K., Han, G.Y., Lee, C.Y., 2012. Comparative evaluation of the HVDC and HVAC links integrated in a large offshore wind farm—an actual case study in Taiwan. IEEE Trans. Ind. Appl. 48, 1639–1648.

De Alegría, I.M., Martín, J.L., Kortabarria, I., Andreu, J., Ereño, P.I., 2009. Transmission alternatives for offshore electrical power. Renew. Sustain. Energy Rev. 13, 1027–1038.

De Decker, Grid Jan, Paul, Kreutzkamp, Achim, Woyte, Carlos Dierckxsens De Decker, J., Kreutzkamp, P., Woyte, A., et al., 2012. „The impact of large-scale offshore electricity transmission: the European project offshore grid. In: Proceedings of the 9th International Conference on the European Energy Market. EEM), pp. 1–8.

Elgerd, O., 1982. Electric Energy Systems Theory: an Introduction", second ed. McGraw-Hill, New York.

Institute of Electrical and Electronics Engineers Inc.. In: Eremia, M., Shahidehpou, M. (Eds.), 2013. Handbook of Electrical Power System Dynamics: Modeling, Stability, and Control". John Wiley & Sons, Inc., ISBN 978-1-118-49717-3

Erlich, I., Shewarega, F., Engelhardt, S., Kretschmann, J., Fortmann, J., Koch, F., 2009. Effect of wind turbine output current during faults on grid voltage and the transient stability of wind parks. In: Proceedings of the IEEE-PES General Meeting. Calgary, Canada; 26–30 July.
Erlich, I., Shewarega, F., Feltes, C., Koch, F.W., Fortmann, J., 2013. Offshore wind power generation technologies. Proc. IEEE 101, 891–905.
Fernández-Guillamón, A., Das, K., Cutululis, N.A., Molina-García Á, 2019. Offshore wind power integration into future power systems: overview and trends. J. Mar. Sci. Eng. 7 (11), 399. https://doi.org/10.3390/jmse7110399.
Garcia-Sanz, M., Houpis, C.H., 2012. Wind Energy Systems". Taylor & Francis Group.
Häring, I., et al., 2017. Towards a generic resilience management, quantification and development process: general definitions, requirements, methods, techniques and measures, and case studies. In: Linkov, I., Palma-Oliveira, J. (Eds.), Resilience and Risk, NATO Science for Peace and Security Series C: Environmental Security. Springer, Dordrecht. https://doi.org/10.1007/978-94-024-1123-2_2.
Holdsworth, L., Jenkins, N., Strbac, G., November 2001. Electrical stability of large, offshore wind farms. In: IEE AC-DC Power Transmission. Conference Publication No. 485, London, pp. 156–161.
Jones, C., et al., 2018. Offshore Wind Sediment Stability Evaluation Framework. Offshore Technology Conference, USA. https://doi.org/10.4043/28711-MS.
Khaitan, S.K., McCalley, J.D., June 2015. Design techniques and applications of cyberphysical systems: a survey. IEEE Syst. J. 9 (2), 350–365. https://doi.org/10.1109/JSYST.2014.2322503.
Kröger, W., Zio, E. (Eds.), 2011. Vulnerable Systems". Springer London, ISBN 9780857296559.
Kulev, N., Reuter, A., Eichhorn, O., Engler, E., Wrede, C., 2019. Nonresilient Behavior of Offshore Wind Farms Due to Cyber-Physical Attacks". Proceedings of 8th REA symposium.
Kumar, D., Chatterjee, K., 2016. A review of conventional and advanced MPPT algorithms for wind energy systems. Renew. Sustain. Energy Rev. 55, 957–970.
Kundur, P., et al., 2004. Definition and classification of power system stability IEEE/CIGRE joint task force on stability terms and definitions. IEEE Trans. Power Syst. 19 (3), 1387–1401, Aug. https://doi.org/10.1109/TPWRS.2004.825981.
Liserre, M., Cardenas, R., Molinas, M., Rodriguez, J., 2011. Overview of multi-MW wind turbines and wind parks. IEEE Trans. Ind. Electron. 58, 1081–1095.
Machowski, J., Bialek, J.W., Bumby, J., 2011. Power System Dynamics: Stability and Control". Wiley, ISBN 9781119965053.
MathWorks. Simscape™ Electrical™ user's guide. Retrieved from. https://www.mathworks.com/help/pdf_doc/physmod/sps/sps_ug.pdf.
MathWorks. Simscape™ Electrical™ user's guide (specialized power systems). Retrieved from. https://www.mathworks.com/help/pdf_doc/physmod/sps/powersys_ug.pdf.
MathWorks. Simulink™ user's guide. Retrieved from. https://www.mathworks.com/help/pdf_doc/simulink/simulink_ug.pdf.
Negra, N.B., Todorovic, J., Ackermann, T., 2006. Loss evaluation of HVAC and HVDC transmission solutions for large offshore wind farms. Elec. Power Syst. Res. 76, 916–927.
Ng, C., Ran, L. (Eds.), 2016. Offshore Wind Farms". Elsevier.
Njiri, J.G., Soeffker, D., 2016. State-of-the-art in wind turbine control: trends and challenges. Renew. Sustain. Energy Rev. 60, 377–393.
Panteli, M., Mancarella, P., September 2017. Modeling and evaluating the resilience of critical electrical power infrastructure to extreme weather events. IEEE Syst. J. 11 (3).
Perelmuter, V., 2017. Renewable Energy Systems: Simulation with Simulink® and SimPowerSystems™". Taylor & Francis, CRC Press, ISBN 978-1-4987-6598-5.
Perveen, Rehana, Kishor, Nand, Mohanty, Soumya R., 2014. Off-shore wind farm development: present status and challenges. Renew. Sustain. Energy Rev. 29, 780–792. https://doi.org/10.1016/j.rser.2013.08.108. ISSN 1364-0321.
Preda, T.-N., 2016. Modelling of Active Distribution Grids for Stability Analysis". Norwegian University of Science and Technology, Dissertation, ISBN 978-82-326-1422-6 (printed ver.).
Rolf, Isermann, 2007. Mechatronic Systems: Fundamentals". Springer Science & Business Media. ISBN 1846282594, 9781846282591.
Sansavini, G., 2017. Engineering Resilience" in Critical Infrastructures, pp. 189–203, 01.
Schaffarczyk, A., 2014. Understanding Wind Power Technology: Theory, Deployment and Optimization". John Wiley & Sons, Ltd.
F. Sill Torres, N. Nikolai, B. Bartosz, M. Meyer, O. Michael and J. Schäfer-Frey, "Indicator-based safety and security assessment of offshore wind farms", Resilience Week (RWS), USA. doi: 10.1109/RWS50334.2020.9241287.
Staggs, J., Ferlemann, D., Shenoi, S., 2017. Wind farm security: attack surface, targets, scenarios and mitigation. Int. J. Crit. InfraStruct. Protect. 17, 3–14. https://doi.org/10.1016/j.ijcip.2017.03.001. ISSN 1874-5482.
Wu, Y.K., Lee, C., Shu, G.H., 3–7 October 2010. Taiwan first large-scale offshore wind farm connection – a real project case study. In: Proceedings of the IEEE Industry Applications Society Annual Meeting. IAS. Article no. 5614524, Category no. CFP10IAS-ART, Code-82826.
Wu, H., Liu, J., Cui, M., Liu, X., Gao, H., 2019. Power grid reliability evaluation considering wind farm cyber security and ramping events. Appl. Sci. 9 (15), 3003. https://doi.org/10.3390/app9153003.
Yan, J., Liu, C., Govindarasu, M., 2011. Cyber intrusion of wind farm SCADA system and its impact analysis. In: 2011 IEEE/PES Power Systems Conference and Exposition, pp. 1–6. https://doi.org/10.1109/PSCE.2011.5772593.
Zhang, Z., Chen, A., Matveev, A., Nilssen, R., Nysveen, A., 2013. High-power generators for offshore wind turbines. Energy Proc. 35, 52–61. ISSN 1876-6102.

Further reading

Francis, R., Bekera, B., 2014. A Metric and Frameworks for Resilience Analysis of Engineered and Infrastructure Systems, vol. 121. Reliability Engineering & System Safety, pp. 90–103.